



Published in final edited form as:

*J Glaucoma*. 2019 March ; 28(3): 265–269. doi:10.1097/IJG.0000000000001188.

## An examination of the frequency of paravascular defects and epiretinal membranes in eyes with early glaucoma using en-face slab OCT images

Maria A. Mavrommatis, BA<sup>1</sup>, Nicole De Cuir, MD<sup>1</sup>, Juan Reynaud, MScE<sup>3</sup>, Carlos Gustavo De Moraes, MD MPH<sup>2</sup>, Daiyan Xin, MD<sup>1</sup>, Rashmi Rajshekhar, BS<sup>1</sup>, Jeffrey M. Liebmann, MD<sup>2</sup>, Robert Ritch, MD<sup>4</sup>, Brad Fortune, PhD<sup>3</sup>, and Donald C. Hood, PhD<sup>1,2</sup>

<sup>1</sup>Dept. of Psychology, Columbia University, New York, NY, USA.

<sup>2</sup>Dept. of Ophthalmology, Columbia University, New York, NY, USA.

<sup>3</sup>Discoveries in Sight Research Lab, Legacy Devers Eye Institute, Portland, OR, USA.

<sup>4</sup>Einhorn Clinical Research Center, New York Eye, and Ear Infirmary, New York, NY, USA

### Abstract

**Purpose:** To examine the frequency of paravascular defects (PDs) and macular epiretinal membranes (ERMs) in eyes categorized as having mild glaucoma or glaucoma suspect using en-face slab analysis of optical coherence tomography (OCT) scans.

**Methods:** 57 glaucomatous eyes, 44 low-risk suspect eyes, and 101 healthy control eyes were included in the study. The 101 glaucomatous and suspect eyes had a mean deviation (MD) better than  $-6$ dB on the 24-2 VF, and a spherical refractive error between  $\pm 6$ D or axial length  $<26.5$ mm. Two OCT-graders masked to eye classification identified ERMs and PDs on en-face slab images of the macula and peripapillary retina using horizontal B-scans and derived vertical B-scans.

**Results:** Glaucomatous eyes had a significantly higher number of PDs and ERMs than healthy controls (PD,  $p < 0.001$ ; ERM,  $p = 0.046$ ) and low-risk glaucoma suspects (PD,  $p = 0.004$ ; ERM,  $p = 0.043$ ). PDs and/or ERMs were present in 16 of 57 (28.1%) glaucomatous eyes, 2 of 44 (4.5%) suspect eyes, and 3 of 101 (3.0%) control eyes. Further, PDs were present in 11 of the 57 (19.3%) glaucomatous eyes, 1 of the 44 (2.3%) suspect eyes and 0 of the 101 (0%) control eyes, ERMs were seen in 7 of the 57 (12.3%) glaucomatous eyes, 1 of the 44 (2.3%) suspects and 3 of the 101 (3.0%) control eyes.

**Conclusions:** Eyes with early glaucoma have a higher frequency of PDs and ERMs than suspects or controls and exhibit PDs even in the absence of ERMs or high myopia.

### PRÉCIS

Early glaucomatous eyes have a significantly higher frequency of paravascular defects (PDs) and epiretinal membranes (ERMs) than glaucoma suspect or control eyes, and they can exhibit PDs in the absence of ERMs or high myopia.

## Keywords

glaucoma; paravascular defects; epiretinal membranes; optical coherence tomography

---

## INTRODUCTION

A paravascular defect (PD) is a separation of the retinal nerve fiber layer (RNFL) from the retinal blood vessel that creates a hole or fissure seen along the vessels.<sup>1-3</sup> Before optical coherence tomography (OCT), PDs had been described in eyes with high myopia.<sup>2</sup> As the use of OCT became more widespread, clinicians began to report cases of PDs in high myopes and eyes with epiretinal membranes (ERMs).<sup>3, 4</sup> Muraoka et al.<sup>5</sup> coined the term paravascular inner retinal defect (PIRD) to describe ‘spindle-shaped’ inner retinal defects that track along blood vessels, but do not necessarily connect to the optic disc. These defects, identified on fundus photographs and confirmed with OCT scans, were associated with high myopia and ERMs. However, eyes with glaucomatous damage were excluded from their study. More recently, using en-face slab imaging, which is described in the methods section, Hood et al.<sup>6</sup> used the term paravascular defect (PD) of the RNFL to include Muraoka et al.’s PIRDs as well as smaller defects that were not seen on fundus photographs and that in some cases were continuous with the optic disc. They observed that these PDs could be associated with glaucomatous damage, as well as with high myopia and ERMs.

Although PDs are associated with certain risk factors, their frequency in the general population remains unclear. Understanding the frequency of PDs becomes particularly interesting in the setting of glaucomatous damage, where both conditions affect the RNFL and tend to occur in similar locations.<sup>4</sup> In particular, PDs most commonly track along the temporal blood vessels and are often continuous with the optic disc.<sup>5</sup> Similarly, glaucomatous damage to the RNFL usually occurs at the superior and inferior disc, creating arcuately shaped defects in the superotemporal and inferotemporal retina. Thus, when there is superotemporal or inferotemporal thinning of the RNFL (detected by OCT, for example), it could be associated with glaucomatous damage or PDs.<sup>6</sup>

ERM is another condition that can affect RNFL. An ERM is a fibrocellular proliferation that typically lies flat against the inner limiting membrane (ILM). If the ERM contracts, it can separate from the underlying inner retina, distort the RNFL, and create a condition sometimes referred to as “surface wrinkling retinopathy.”<sup>7</sup> ERM contraction, similar to PDs, can affect RNFL thickness in regions associated with glaucomatous damage.<sup>8</sup> For example, contracted ERMs can affect the computer-generated segmentation of the RNFL within the temporal arcade.<sup>8</sup>

Recently, we showed that en-face slab images can be used to distinguish glaucomatous damage from PDs and/or ERMs.<sup>6</sup> The purpose of this study was to use en-face slab analysis of OCT scans to examine the frequency of PDs and macular ERMs in eyes categorized as mild glaucoma or glaucoma suspect as compared to healthy controls.

## MATERIALS AND METHODS

### Subjects

101 eyes of 101 patients with abnormal or suspicious looking discs based upon stereo photographs were included in the study ( $57.1 \pm 13.8$  years). They all had a mean deviation (MD) better than  $-6$  dB on the 24-2 visual field (VF), and a spherical refractive error between  $\pm 6$  D. All eyes were free of other disease processes that could affect the VF and had no significant cataract as defined by the Lens Opacities Classification System (III).<sup>9</sup> These 101 eyes were classified as glaucomatous eyes (57) or low-risk (“healthy”) suspect eyes (44) as previously described.<sup>10</sup> The latter referred to here as “suspect eyes,” were classified by glaucoma specialists as “healthy” (i.e. without glaucomatous damage) although their discs were abnormal and/or anomalous. 101 eyes from 101 healthy individuals served as controls ( $55.6 \pm 9.6$  years). These eyes were a subset of a larger group of over 400 healthy eyes included in a reference database study by the OCT device manufacturers (data provided by Topcon, Inc., Tokyo, Japan). One eye was chosen based on age similarity to be the control eye for each of the 101 patients; they had a best-corrected visual acuity of 20/40 or better and an intraocular pressure less than 21 mm Hg. Eyes with narrow angles or any ocular pathology or glaucomatous visual field abnormalities on a visual field test performed using the SITA Standard 24-2 strategy were not included. Participants also were required to be free from a significant medical history that could affect the test results.

This prospective study was approved by the Institutional Review Board of the Columbia University and New York Eye and Ear Infirmary of Mount Sinai and followed the tenets of the Declaration of Helsinki. Informed consent was obtained from each subject after explanation of the nature and possible consequences of participation in the study.

### En-face slab images

All eyes had wide-field, swept-source OCT (ssOCT) cube scans ( $9 \times 12$  mm, 256 B-scans, 512 A-scans; DRI-OCT, Topcon, Inc., Tokyo, Japan). Special purpose software<sup>11</sup> was used to generate en-face projection images based on reflectance intensity for a fixed slab of the widefield ssOCT cube scans.

Figure 1A shows a slab (shaded green) with a fixed thickness of  $52 \mu\text{m}$  (20 voxels). The vitreous/ILM serves as the proximal border. For each of the 256 B-scans, the axial information for each pixel of the slab has been averaged and is projected in an en-face view to form an average voxel projection (AVP) image (Fig. 1B). Note, the segmentation of the ILM was automatically generated by a computer algorithm and were not manually corrected. A slab thickness of  $52 \mu\text{m}$  was used because it has been shown to be small enough to highlight local differences in reflectance intensity and large enough to benefit from averaging a greater number of voxels in depth.<sup>11</sup>

### Identification of PDs and ERMs

Two OCT-experienced authors, masked to clinical classification, identified PDs and ERMs on en-face slab images with additional scrutiny of horizontal and derived vertical B-scans. On en-face slab image, PDs were identified as dark regions adjacent to blood vessels (Fig.

2A, superior vessel), while on horizontal B-scans and derived vertical B-scans, these regions appeared as holes or fissures adjacent to blood vessels (Fig. 2A, orange insets). To be considered a PD, breaks in the RNFL had to extend over at least 3 B-scans. To quantify the length of the PD, the region of the blood vessel adjacent to the PD was marked on the en-face image.

ERMs with separation from the ILM were identified within the temporal arcade. On en-face slab images, macular ERMs were identified by dark regions (Fig. 2B), which corresponded to separation from the ILM on horizontal B-scans and derived vertical B-scans (Fig. 2B, magenta insets). The two graders agreed in 99 of the 101 (98.0%) patient eyes for identification of macular ERMs and in 93 of 101 eyes (92.1%) for PDs. Agreement was 100.0% (101 of 101 eyes) for identification of macular ERMs and 99.0% (100 of 101 eyes) for PDs in the control group. After discussion between the two raters of these few discrepancies, consensus (100% agreement) was achieved for identification of macular ERMs and PDs for both the experimental and control groups.

### Statistical Analysis

Data was analyzed using both univariable and multivariable logistic regression analysis (StataCorp. 2015. *Stata Statistical Software: Release 14*. College Station, TX: StataCorp LP) as well as chi-square analysis.

### RESULTS:

Glaucomatous eyes had a significantly higher number of PDs and ERMs than healthy subjects and suspects [PD:  $p < 0.001$  and  $p = 0.004$ , respectively, for glaucoma (GL) vs healthy control (HC) and glaucoma suspect (GS); ERM:  $p = 0.046$  and  $p = 0.043$  (chi-square analysis)]. PDs and/or ERMs were seen in 16 of 57 (28.1%) glaucomatous eyes, 2 of 44 (4.5%) suspects, and 3 of 101 (3.0%) control eyes (Table 1). Further, PDs were seen in 11 of the 57 (19.3%) glaucomatous eyes, 1 of the 44 (2.3%) suspects and 0 of the 101 (0.0%) controls eyes, while ERMs were seen in 7 of the 57 (12.3%) glaucomatous eyes, 1 of the 44 (2.3%) suspects and 3 of the 101 (3.0%) controls eyes.

Figure 2A shows an example of a PD. On the en-face image, the red line indicates the portion of the blood vessels with the PD. Note, the ‘trench-like’ appearance of the PD as it tracks along the blood vessel. The orange boxes are horizontal and derived vertical B-scan image, which correspond to the same color dashed line on the en-face image. On both horizontal and vertical B-scans, the PD appears as a hypointense ‘hole’ adjacent to both sides of the blood vessel.<sup>6</sup>

Figure 2B shows an example of an ERM (region above the red arrow). On the en-face image, the magenta boxes represent horizontal and derived vertical B-scan images, which correspond to the same color dashed line on the en-face image. The vertical and horizontal B-scans show thickening of the ILM with irregular separation from the retina, which contributes to its ‘wrinkled’ appearance on en-face.

### Paravascular Defects

PDs were not associated with ERMs in the 57 glaucomatous eyes. Only 2 of the 11 (18.2%) glaucomatous eyes with PDs had ERMs. While previous studies have shown that eyes with PDs often have ERMs,<sup>1, 5, 12, 13</sup> it is likely due to the fact that both PDs and ERMs have been associated with high myopia.<sup>5</sup> However, in this study, all eyes had a spherical refractive error better than -6D.

On the other hand, we recently argued that PDs in eyes with glaucomatous damage can appear near arcuate defects of the RNFL.<sup>6</sup> Of the 11 glaucomatous eyes with PDs, 5 eyes had PDs within an arcuate RNFL defect (Table 1). En-face slab images for 4 of these eyes are shown in Figure 3. Of these 5 eyes, 4 did not have ERMs while the fifth eye (GL 16) had a small ERM (Fig. 3 yellow arrow). The PDs, which have been confirmed on horizontal B-scans (orange insets) and outlined in red, are located within arcuate defects (white arrows). All RNFL arcuate defects were confirmed by circumpapillary frequency domain OCT scans and corresponding defects on 24-2VF (data not shown).

### Epi-retinal Membranes

ERMs were seen in 7 of the 57 glaucomatous eyes, one of the 44 suspect eyes, and 3 of the 101 control eyes. In general, the ERMs were related to older age according to univariable logistic regression ( $p = 0.009$ ). However, when age was taken into account by multivariable logistic regression, glaucomatous eyes still had a higher frequency of macular ERMs than did suspect or controls ( $p = 0.037$ ).

### DISCUSSION:

Our purpose was to use en-face slab analysis of OCT scans to examine the frequency of PDs and macular ERMs in eyes categorized as mild glaucoma or glaucoma suspect. Glaucomatous eyes were more likely to have either PDs or ERMs than suspects and controls.

ERMs were also more prevalent in glaucomatous eyes than in suspects and controls. As expected, ERMs increased in frequency with age, however even after accounting for age by multivariable regression, glaucomatous eyes still had a significantly greater frequency of ERMs. The 7 ERMs identified in glaucomatous eyes resembled the ERM in the suspect eye in appearance on en-face and in location in the macular region. Similar to the results of Miyoshi et al.,<sup>13</sup> ERMs in eyes with PD tended to occur within the temporal arcade and were not continuous with PDs.

The PDs identified in glaucomatous eyes (19.3% frequency) had a similar appearance and characteristics to PDs and PIRDs described by other studies.<sup>5, 6</sup> In particular, Muraoka et al.<sup>5</sup> noted that PIRDs are most often adjacent to temporal blood vessels, tend to favor the superior temporal region over the inferior temporal region, and are more commonly adjacent to veins than arteries. Hood et al.<sup>6</sup> reported a similar trend. In the current study, PDs were adjacent to major blood vessels in 11 of 16 glaucomatous eyes and all but one of these vessels was located in the temporal region. Specifically, 6 PDs (54.5%) were adjacent to superotemporal blood vessels, 3 (36.4%) were adjacent to inferotemporal vessels, and 1

(9.1%) was adjacent to an inferonasal vessel. PDs were more commonly found adjacent to veins (13/16) than arteries (3/16).

The results of this study appear to contradict those reported in a recently published manuscript by Osaka et al.<sup>14</sup> Osaka and colleagues investigated the frequency and characteristics of paravascular inner retinal abnormalities (PIRAs), comparable to our PDs, in specifically healthy eyes using similar OCT scans. They reported PIRAs in 77 (43.3%) eyes, 71 (39.9%) of which were inner retinal cystoid or fissure-like spaces that had no connection to the vitreous cavity, and four (2.2%) of which were inner retinal cleavages with openings to the vitreous cavity. Note, however, that there currently exists no consensus on the naming, categorization, or identification of these inner retinal defects that form and track along blood vessels. In the case of Osaka et al., paravascular abnormalities were classified according to a pre-existing report<sup>13</sup> that expanded the criteria of paravascular abnormalities to include different grades of PIRs, such that cystoid or fissure-like spaces with no openings to the vitreous cavity were distinguished from cleavages with openings to the vitreous. Note that only 2.2% of patients in the study by Osaka et al. exhibited the kind of paravascular cleavage most similar to those in Muraoka et al.'s original paper<sup>5</sup> and Hood et al.'s previous results.<sup>6</sup> The additional 39.9% of patients in Osaka et al.'s study exhibited far smaller lesions that may or may not belong in this categorization. Thus, we suggest that the results of the current study do not contradict those of Osaka et al.; rather, they use different language and definitions to describe similar pathology.

Furthermore, the results of this study suggest that glaucoma may be an independent risk factor for PDs. PDs have been associated with ERMs and high myopia,<sup>5</sup> however, glaucomatous eyes with PDs need not have high myopia or ERMs.<sup>6</sup> High myopia was excluded from the present study and only 2 of 11 (18.2%) glaucomatous eyes with PDs had ERMs. In eyes with glaucomatous damage, but without ERM or high myopia, PDs can appear within arcuate defects. 5 glaucomatous eyes had PDs within arcuate defects. Similar findings were seen in a recent study by Hood et al.<sup>6</sup> They described six glaucomatous eyes that had PDs within an arcuate defect. Notably, none of these eyes had ERMs and only one of the six eyes had high myopia.

The findings of this study are limited to eyes with early glaucoma and without high myopia. For example, it is to be expected that eyes with high myopia will have a higher frequency of ERM and PDs.<sup>5</sup> Further, we noted an association between PDs and glaucomatous arcuate defects, however, because of the study's cross-sectional design, it remains unclear whether the arcuate defect preceded or followed the formation of a PD. Further study is indicated to determine the sequence and relationship of these findings.

In conclusion, glaucomatous eyes have a higher incidence of PDs and ERMs than healthy controls. Because PDs and glaucomatous damage tend to occur in similar locations (temporal retina) and each can result in VF defects,<sup>3</sup> PDs can masquerade as glaucomatous damage.<sup>3, 4</sup> In eyes with ERM and PDs, clinicians should be careful not to confuse these structural abnormalities with changes due to glaucoma. En-face imaging, which is becoming widely available in commercial OCT machines, is an effective technique for distinguishing the effect of these three conditions – glaucoma, ERMs, and PDs – on the RNFL.



## Acknowledgments:

**Funding sources:** Supported by National Institutes of Health Grant R01-EY02115 (DCH) and NIH R01-EY019327 (BF)

Grant Support: NIH R01-EY02115 and NIH R01-EY019327, The Crowley Family Fund of the New York Eye and Ear Infirmary of Mount Sinai (New York, New York), The Lary Stromfeld Research Fund of the New York Eye and Ear Infirmary of Mount Sinai.

## REFERENCES

1. Liu H-Y, Hsieh Y-T, Yang C-M. Paravascular abnormalities in eyes with idiopathic epiretinal membrane. *Graefe's Archive for Clinical and Experimental Ophthalmology*. 2016;254:1723–1729.
2. Chihara E, Chihara K. Apparent cleavage of the retinal nerve fiber layer in asymptomatic eyes with high myopia. *Graefe's Archive for Clinical and Experimental Ophthalmology*. 1992;230:416–420.
3. Komeima K, Kikuchi M, Ito Y, Terasaki H, Miyake Y. Paravascular inner retinal cleavage in a highly myopic eye. *Arch Ophthalmol*. 2005;123:1449–1450. [PubMed: 16219744]
4. Hwang YH, Kim YF, Kim HK, Sohn YH. Characteristics of eyes with inner retinal cleavage. *Graefes Arch Clin Exp Ophthalmol*. 2015;253(2):215–220. [PubMed: 24939282]
5. Muraoka Y, Tsujikawa A, Hata M, et al. Paravascular inner retinal defect associated with high myopia or epiretinal membrane. *JAMA Ophthalmology*. 2015;133:413–420. [PubMed: 25611517]
6. Hood DC, De Cuir N, Mavrommatis MA, et al. Defects Along Blood Vessels in Glaucoma Suspects and Patients. *Invest Ophthalmol Vis Sci*. 2016;57:1680–1686. [PubMed: 27054521]
7. Bu S-C, Kuijjer R, Li X-R, Hooymans JMM, Los LI. IDIOPATHIC EPIRETINAL MEMBRANE. *Retina*. 2014;34:2317–2335. [PubMed: 25360790]
8. Rüfer F, Bartsch JJ, Erb C, Riehl A, Zeitz PF. Epiretinal membrane as a source of errors during the measurement of peripapillary nerve fibre thickness using spectral-domain optical coherence tomography (SD-OCT). *Graefe's Archive for Clinical and Experimental Ophthalmology*. 2016;254:2017–2023.
9. Wong WL, Fau Li X - Li J, Fau Li J - Cheng C-Y, et al. Cataract conversion assessment using lens opacity classification system III and Wisconsin cataract grading system. *Investigative Ophthalmology & Visual Science*. 2013;54:208–207.
10. Hood DC, De Cuir N, Blumberg DM, et al. A Single Wide-Field OCT Protocol Can Provide Compelling Information for the Diagnosis of Early Glaucoma. *Translational Vision Science & Technology*. 2016;5:4.
11. Hood DC, Fortune B, Mavrommatis MA, et al. Details of Glaucomatous Damage Are Better Seen on OCT En Face Images Than on OCT Retinal Nerve Fiber Layer Thickness Maps. *Invest Ophthalmol Vis Sci*. 2015;56:6208–6216. [PubMed: 26426403]
12. Hood DC, Raza AS. Method for comparing visual field defects to local RNFL and RGC damage seen on frequency domain OCT in patients with glaucoma. *Biomedical Optics Express*. 2011;2.
13. Miyoshi Y, Tsujikawa A, Manabe S, et al. Prevalence, characteristics, and pathogenesis of paravascular inner retinal defects associated with epiretinal membranes. *Graefe's Archive for Clinical and Experimental Ophthalmology*. 2016;1–9.
14. Osaka R, Manabe S, Miyoshi Y, et al. Paravascular inner retinal abnormalities in healthy eyes. *Graefe's Archive for Clinical and Experimental Ophthalmology*. 2017;255:1743–1748.

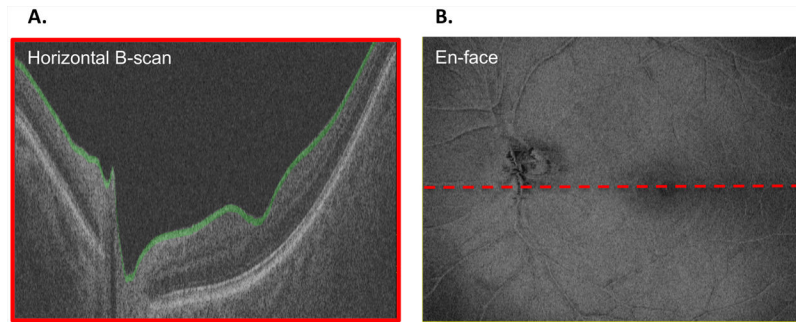


**Figure 1:**

(A) B-scan (horizontal: vertical ratio of 1:6) through the optic disc of a left eye showing a slab (shaded green) with a fixed thickness of  $52\ \mu\text{m}$  (20 voxels) with the vitreous/ILM as the proximal border. (B) En-face image of the averaged voxel projection (AVP) of the  $52\ \mu\text{m}$  slab shown in (A) across all of the 256 B-scans. The dashed red line shows the location of the B-scan in panel A.



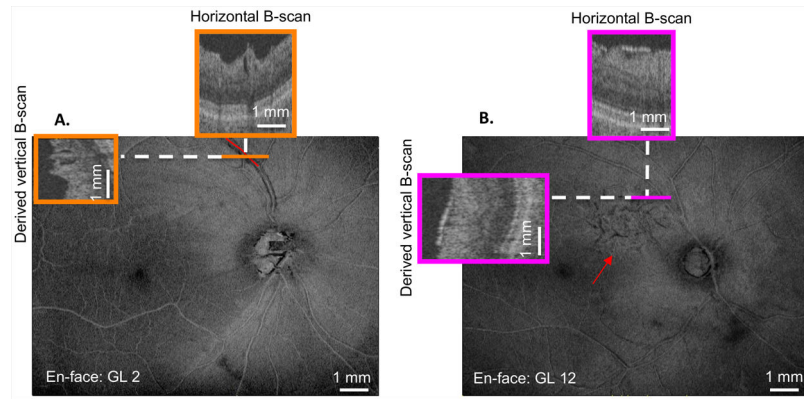


**Figure 2:**

(A) En-face image of the 52  $\mu\text{m}$ -slab average voxel projection (AVP) of GL 2. Orange insets indicate the horizontal (upper) and derived vertical (left) B-scans at the location indicated by the solid orange line. The red line along the superior vessel indicates the presence and length of the paravascular defect (PD). (B) En-face image of the 52  $\mu\text{m}$ -slab AVP of GL 12. Magenta insets indicate the horizontal (upper) and derived vertical (left) B-scans at the location indicated by the solid magenta line. The red arrow indicates the inferior border of the epiretinal membrane (ERM) on the en-face projection.

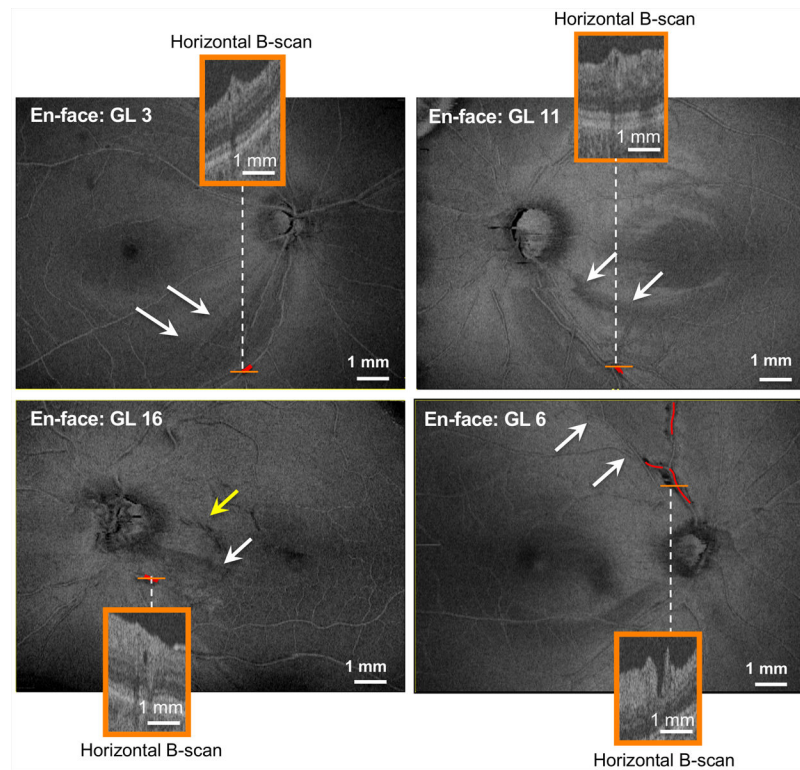


**Figure 3:** En-face images of 4 eyes (GL 3, GL 6, GL 11, and GL 16) with PDs. The orange insets are the horizontal B-scans at the location indicated by the solid orange line in each image. The red lines indicate the location and length of the respective PDs, the white arrows demonstrate regions of arcuate RNFL damage, and the yellow arrow in en-face image of GL 16 indicates the presence of a small epiretinal membrane (ERM).

**Table 1:**

Clinical data for the 16 glaucomatous (GL) eyes, 2 glaucoma suspect (GS) eyes, and 3 healthy control (HC) eyes that exhibited one or more of the following: epiretinal membranes (ERMs), paravascular defects (PDs), and arcuate retinal nerve fiber layer (RNFL) defect. Note that no control eyes exhibited PDs.

| GLAUCOMA (n=57) |          |                      |      |     |                               |                              |
|-----------------|----------|----------------------|------|-----|-------------------------------|------------------------------|
|                 | Age (yr) | Refractive Error (D) | ERMs | PDs | PD within Arcuate RNFL Defect | Total PD Length per Eye (mm) |
| GL 1            | 78.1     | 1.5                  | x    |     |                               | -                            |
| GL 2            | 74.9     | n/a                  |      | x   |                               | 1.506                        |
| GL 3            | 57.3     | -1                   |      | x   | x                             | 0.536                        |
| GL 4            | 72.8     | 2.75                 | x    | x   |                               | 2.922                        |
| GL 5            | 56.2     | -4.5                 |      | x   |                               | 1.642                        |
| GL 6            | 52.3     | -0.5                 |      | x   | x                             | 2.839                        |
| GL 7            | 57.3     | -3                   |      | x   |                               | 1.348                        |
| GL 8            | 66.6     | -2.25                | x    |     |                               | -                            |
| GL 9            | 66.9     | 2                    | x    |     |                               | -                            |
| GL 10           | 73.5     | -2.5                 | x    |     |                               | -                            |
| GL 11           | 35.9     | -2.5                 |      | x   | x                             | 0.251                        |
| GL 12           | 59.2     | -3.5                 | x    |     |                               | -                            |
| GL 13           | 67.7     | 2                    |      | x   |                               | 2.835                        |
| GL 14           | 62.7     | 1.75                 |      | x   | x                             | 0.876                        |
| GL 15           | 65.4     | 1.5                  |      | x   |                               | 2.113                        |
| GL 16           | 75.3     | 1.25                 | x    | x   | x                             | 0.467                        |

| SUSPECTS (n=44) |          |                      |      |     |                               |                              |
|-----------------|----------|----------------------|------|-----|-------------------------------|------------------------------|
|                 | Age (yr) | Refractive Error (D) | ERMs | PDs | PD within Arcuate RNFL Defect | Total PD Length per Eye (mm) |
| GS 1            | 63.9     | 1.5                  | x    |     |                               | -                            |
| GS 2            | 63.5     | -2.25                |      | x   |                               | 0.903                        |

| HEALTHY CONTROLS (n=111) |          |                      |      |     |                               |                              |
|--------------------------|----------|----------------------|------|-----|-------------------------------|------------------------------|
|                          | Age (yr) | Refractive Error (D) | ERMs | PDs | PD within Arcuate RNFL Defect | Total PD Length per Eye (mm) |
| C1                       | 65.1     | n/a                  | x    |     |                               |                              |
| C2                       | 65.6     | n/a                  | x    |     |                               |                              |
| C3                       | 65.2     | n/a                  | x    |     |                               |                              |